Notes on Combined Milankovitch and Tidal Theory *

Carl Wunsch

Preliminary Version

1 Gravitational Tides

One of the central elements of all discussions of low frequency climate change is the hypothesis that changes in the earth-sun orbital configuration influencing the solar radiation incident on the earth, has important consequences. This hypothesis has become known as the Milankovitch theory; its history is well-described by Imbrie and Imbrie (1986). A better known physical system dependent upon orbital configurations is the ordinary gravitational tides. In practice, the problem of tides and of Milankovitch are very closely related, and it is interesting to discuss them together, both because it is easy, and because the tides have recently become a center of attention for their possible role in climate change. One can have a nearly unified description.

Milankovitch theory is in some ways much simpler than the tidal problem, because it involves only the relative positions of the sun and earth, whereas the tides also involve the moon—whose motion is extremely complicated. On the other hand, the earth is opaque to solar radiation, whereas it is "transparent" to gravitational forcing, and the opacity renders that part of the insolation forcing discussion more complicated. Despite these differences, several hundred years of experience in understanding gravity tides in the ocean and atmosphere is also a good background for understanding how to determine the response of the climate system to the analogous insolation forcing.

The fundamental framework for discussing both tides and solar radiation is the idea that the nearly spherical earth is in an essentially elliptical orbit about the sun. In practice, it is simpler, and entirely accurate, to take a Ptolemaic view and regard the sun as in orbit about the earth, and we will mostly use that vocabulary. Let us begin with a discussion of solar tides, assuming the moon to be absent.

A straightforward derivation of the tidal potential is given by Lamb (1932) and in the Appendix to Munk and Cartwright (1966). The fundamental positional astronomy is described by

*orbital.tex, July 8, 2004

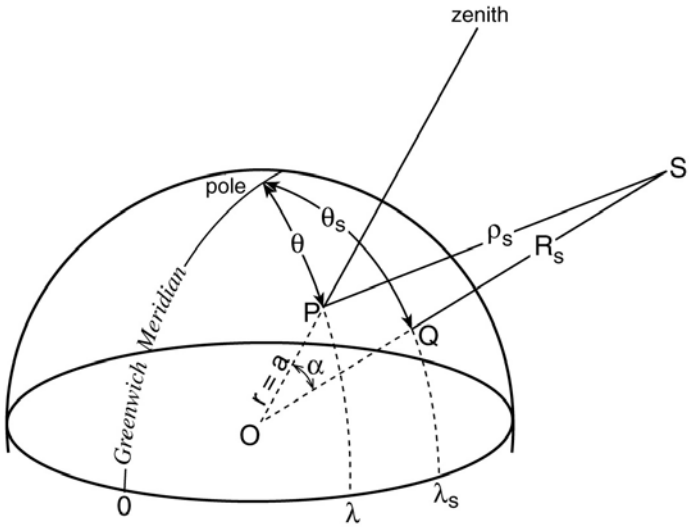

Figure 1: Geometry of the subsolar point Q, relative to that of an observer at P. Only the angle α relative to the center of the earth, and the distance ρ_S are required to calculate the gravitational forcing or insolation at P. (Adapted from Munk and Cartwright, 1966).

Smart (1962), Green (1985), and Anonymous (1961). Astronomers use many different coordinate systems, time measurements, and notations. A good elementary introduction can be found in Bowditch (1962, and later editions). Consider the geometry of Fig. 1 showing an observer at point P with longitude λ, co-latitude θ, and distance r from the center of the earth (most often the earth's radius, $r = a$). The sun is at S, at a distance R_S from the center of the earth and a distance ρ_S (not to be confused with density) from the observer. The solar mass is M_S. For the observer at P, the disturbing gravitational potential of the sun is,

$$V_S = \frac{GM_S}{\rho_S}, \tag{1}$$

where G is the gravitational constant. Let α be the angle, shown between the observer's vertical (the "zenith") and the line connecting the solar position to the center of the earth. Then,

$$V_S = \frac{GM_S}{\rho_S} = \frac{GM_S}{R_S\left(1 - 2\left(r/R_S\right)\cos\alpha + \left(r/R_S\right)^2\right)^{1/2}}. \tag{2}$$

The ratio, r/R_S is the "solar parallax" and is a very small number. Expanding (2) in the parallax, we obtain,

$$V_S = \frac{GM_S}{R_S}\sum_{n=0}^{\infty}\left(\frac{r}{R}\right)^n P_n\left(\cos\alpha\right) = \frac{GM_S}{R_S}\left(1 + \frac{r}{R_S}\cos\alpha + \left(\frac{r}{R_S}\right)^2\left[\frac{3}{2}\cos^2\alpha - \frac{1}{2}\right] + ...\right), \tag{3}$$

where the $P_n(\cos\alpha)$ are the ordinary Legendre polynomials ($P_0 = 1,\ P_1(\cos\alpha) = \cos\alpha,\ P_2(\cos\alpha) = (3/2)\cos^2\alpha - (1/2)$,....

Now the first term is a constant and so has no gradient and produces no force; it can be safely dropped. The gradient of the second term in a spherical coordinate system (r, α, β) (that is with the pole at the subsolar point, so that the observer's co-latitude in that coordinate system is α), is easy to compute, and is just,

$$\frac{GM_S}{R_S}\nabla\left(\frac{r}{R_S}\cos\alpha\right) = \frac{GM_S}{R_S^2}(\cos\alpha,\ -\sin\alpha,\ 0) \tag{4}$$

has a constant magnitude, and is directed toward the sun. It represents the net attraction of the earth by the sun; when multiplied by the earth's density $\rho(\alpha, \beta, r)$ and integrated over the sphere $(0 \le r \le a, 0 \le \alpha \le \pi, 0 \le \beta \le 2\pi)$, it is readily found to have magnitude, $GM_E\, M_S/R_S^2$ where M_E is the earth's mass. The earth does not fall into the sun, and so this force is necessarily balanced by the centrifugal motion of the earth about the sun (see Fig. 2). We are thus left with the third and higher order terms of Eq. (3) or,

$$V_S = \frac{GM_S}{R_S}\left[\left(\frac{r}{R_S}\right)^2\left(\frac{3}{2}\cos^2\alpha - \frac{1}{2}\right) + \left(\frac{r}{R_S}\right)^3 P_3(\cos\alpha) + ...\right] \tag{5}$$

Expression (5) can be simplified a bit. First, note that g, earth's gravity at the surface is,

$$g = \frac{GM_E}{a^2}, \tag{6}$$

where M_E is the earth's mass, and a is it's radius (in spherical approximation). So, $G = a^2 g/M_E$ and,

$$\frac{V_S}{g} = \frac{a^2}{R_S}\frac{M_S}{M_E}\left[\left(\frac{r}{R_S}\right)^2\left(\frac{3}{2}\cos^2\alpha - \frac{1}{2}\right) + ...\right]. \tag{7}$$

Setting $r = a$, we have

$$\frac{V_S}{g} = a\frac{M_S}{M_E}\left[\left(\frac{a}{R_S}\right)^3\left(\frac{3}{2}\cos^2\alpha - \frac{1}{2}\right) + \left(\frac{a}{R_S}\right)^4 P_3(\cos\alpha) + ...\right], \tag{8}$$

at the surface. The surfaces V_S/g =constant are rotationally symmetric ellipsoidal bulges pointing at the subsolar point and at the antipodal point. Physically, the gravitational attraction of the sun is larger than the outward centrifugal force on the side of the earth nearest the sun with a net attraction toward the sun, but on the far-side, the gravitational force is weaker than the centrifugal force, and the apparent gravity is directed away from the sun. An observer on the rotating earth moves in and out of a bulge twice/day, and unless the sun is over the equator, one bulge will appear larger than the other (Fig. 3). This geometric effect is the origin of the

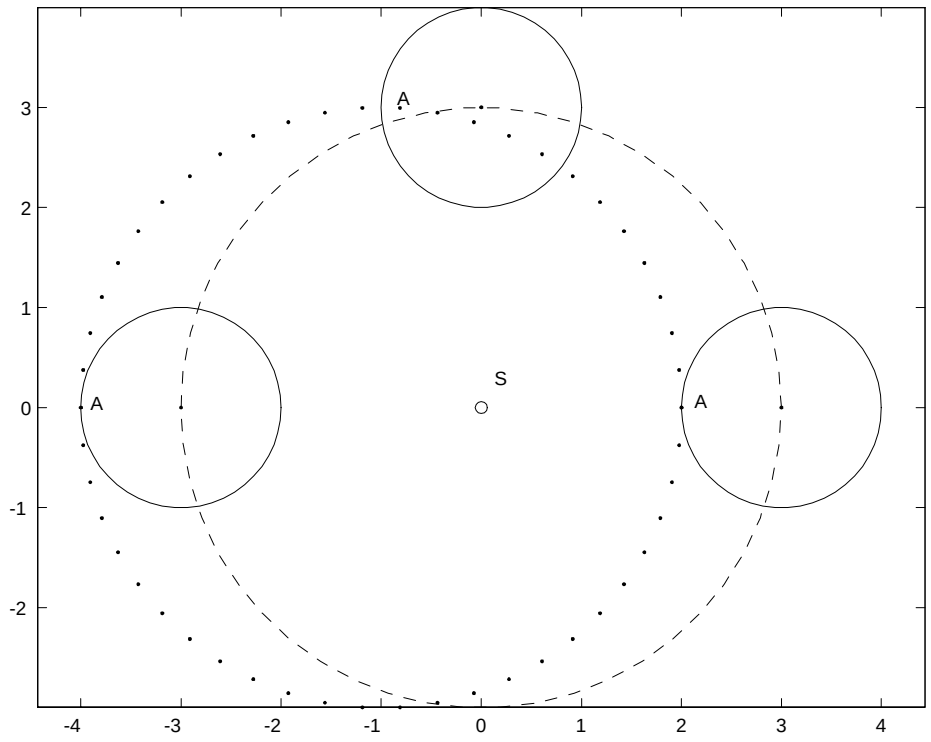

Figure 2: Schematic (after George Darwin) of orbital geometry. For a non-spinning earth in orbit about the sun at S, all points in and on the earth, e.g. A, move in a circle of common diameter, albeit about different centers. Thus all points on the earth experience an identical centrifugal force. The spin motion is simply superimposed, carrying the observer through 360 degrees each day.

– – – – – – – – – – – – – – – –

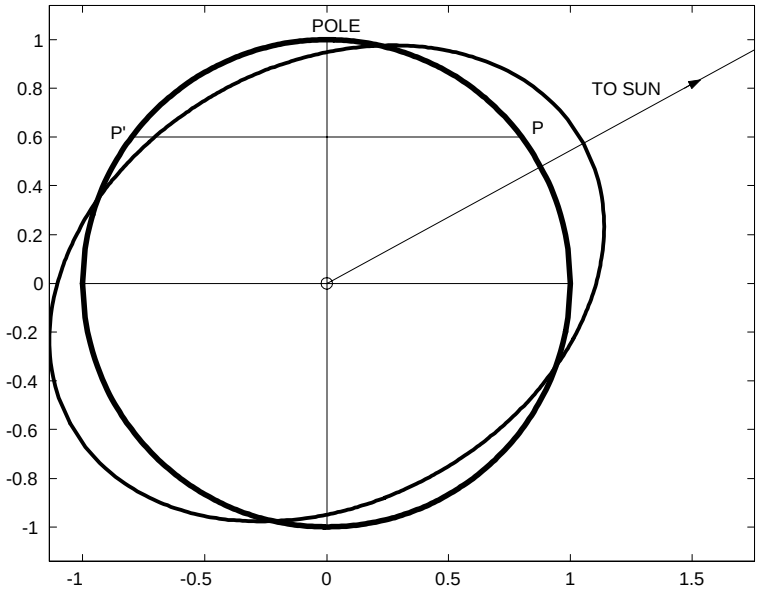

Figure 3: Geometry of the tidal disturbing potential in a plane passing through the pole, center of the earth, and the center of the sun. An observer at P passes through the disturbing potential at a fixed latitude, and hence sees a larger bulge during one part of the cycle than in the other. The difference is the origin of the diurnal tides. At the equinoxes, the effect vanishes as it always does for an observer on the equator.

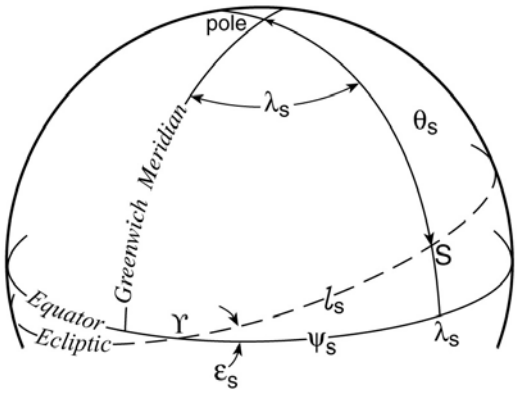

Figure 4: Latitude and longitude of the subsolar point in Greenwich coordinates (λ_s, θ_s). Angles l_s, ψ_s are measured from the vernal equinox Υ. (Adapted from Munk and Cartwright, 1966).

---

dominant semidiurnal, and the diurnal component tide, the latter making one side of the bulge look greater than the other to the observer. See the references.

Eq. (8) is still written in a coordinate system based upon the sub-solar point, and for it to be useful, we need it in ordinary latitude and longitude. Consider Fig. 4 defining the position of the sub-solar point in Greenwich coordinates. θ_S is the co-latitude of the instantaneous sub-solar point, and λ_S is the Greenwich longitude of the instantaneous sun measured from the point (angle) Υ, and which is defined below. From elementary spherical trigonometry we have,

$$\cos\alpha = \cos\theta_S \cos\theta + \sin\theta_S \sin\theta \cos\left(\lambda_S - \lambda\right). \tag{9}$$

(Eq. 9 is a special case of the so-called addition theorem for change of coordinate in spherical harmonics.) Unfortunately, there is a wide variety of notations in use. Substituting (9) into (8), and doing a bit of manipulation, we obtain,

$$\begin{aligned} \frac{V_S}{g} &= \frac{3}{2}H\left(\cos^2\theta_S - \frac{1}{3}\right)\left(\cos^2\theta - \frac{1}{3}\right) + \frac{1}{2}H\sin\left(2\theta_S\right)\sin\left(2\theta\right)\cos\left(\lambda_S - \lambda\right) \\ &\quad + \frac{1}{2}H\sin^2\theta_S \sin^2\theta\cos 2\left(\lambda_S - \lambda\right) + ..., \\ H &= \frac{3}{2}\frac{M_S}{M_E}\left(\frac{a}{R_S}\right)^3. \end{aligned} \tag{10}$$

There is an equivalent expansion explicitly in spherical harmonics. Note that θ, λ remain time independent (observer's co-latitude and longitude). The three terms of (10) as seen by observers with different θ, λ is displayed in Fig. 5.

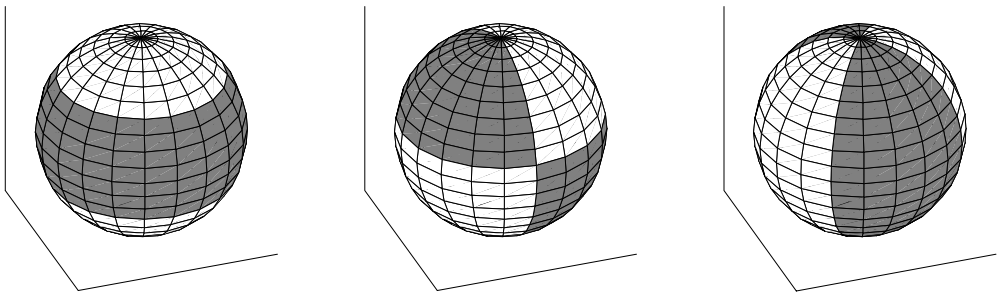

Figure 5: The three terms of Eq. (10), as a function of θ, λ. Panel on the left has no λ dependence, and is the structure of the long-period tides. Middle panel travels eastward and produces the diurnal tides, and the right panel also travel eastwards but produces semi-diurnal tides. The three structures are proportional to spherical harmonics $Y_2(\theta), Y_2^1(\theta,\lambda), Y_2^2(\theta,\lambda)$ respectively.

Eq. (10) provides the basic structure of the most important tidal lines (some higher order terms, represented by the ellipsis, ..., are usually carried along in standard representations, but they are significantly weaker, being proportional to the solar parallax to the fourth power or higher). The first term has no dependence upon λ_S, which is called the "hour-angle" of the sun. Thus its time-dependence is controlled by changes in the solar co-latitude θ_S, and in the solar-radius R_S (in H). Because $\cos^2\theta_S = (1/2)(1+\cos 2\theta_S)$, and θ_S today varies between $\pm 23.5^\circ$ over the year, the trigonometric term has a dominant 6 month periodicity. With the sun moving in an ellipse, R_S will also vary with an annual periodicity; its reciprocal will have an annual period plus all of its harmonics.

The second term on the right contains a term in $\cos(\lambda_S - \lambda)$. Because λ_S changes by 360° in one day, the dominant periodicity will be 24 hours. This term thus gives rise to the solar diurnal tides. Notice that the term vanishes for $\theta = \pi/2$, that is on the equator. The term is also modulated by $\sin(2\theta_S)$, and any variation in R_S throughout the year. The last term is dominated by the time change in $\cos 2(\lambda_S - \lambda)$ and will have a 12 hour period; these are the solar semi-diurnal tides.

Some terms of (10) are time-independent, producing a permanent tidal deformation of the earth, and which is important in defining the reference surfaces for satellite altimetry and geodesy.

1.1 Splitting

Consider the product of two cosines (or of a sine and cosine, etc.) in time,

$$\cos(2\pi s_1 t)\cos(2\pi s_2 t) = \frac{1}{2}\cos(2\pi(s_1 - s_2)t) + \frac{1}{2}\cos(2\pi(s_1 + s_2)t) \tag{11}$$

that is, the product is the same as two cosines in which s_1 is "split" into two new frequencies, $s_1 \pm s_2$. So for example, the second term on the right in (10) is the product of a cosine of a frequency of 1 cycle/day ($\cos(\lambda_S - \lambda)$), and of a sinusoid of frequency 2 cycles/year ($\sin 2\theta_S$). Thus this term can be re-written (left to the reader or the references) as the sum of two terms, one at one cycle/day plus 2 cycles/year and one cycle/day minus 2 cycles/year. Each of these two terms is also multiplied by H which is proportional to $1/R_S^3$, and which one can anticipate will vary at one cycle/year, and with all of its overtones as well. So each of the two terms in (11), in will be *re-split* by one cycle/year and all integer multiples of this frequency. The various products of time dependent sinusoids is the origin of the splitting of the tidal lines into many neighboring frequencies; for the sun, the frequencies are generally separated by integer multiples of one cycle/year. Because one cycle/year is a much smaller frequency than one or two cycles/day, the lines tend to cluster narrowly about one and two cycles/day.

1.2 Solar Motion

It is useful to understand a bit about how astronomers specify R_S, θ_S, λ_S. Consider by way of example, the motion of the sun in its elliptical orbit. In the formulas above, λ_S is not an angle which changes uniformly with time, because the angular movement of a body in an ellipse is not uniform. Consider Fig. 6 (adapted from Smart, 1962, p. 111), The position of the sun in the ellipse is given by its radius, R_S, and the angle v, called the "true anomaly". Kepler's Second Law says that in an elliptical orbit, "equal areas are swept out in equal time", but this implies that the rate of change of v varies with time, and is inconvenient to compute. They prefer to use instead the angle E, called the "eccentric anomaly" which can then in turn, be related to another angle, called the "mean anomaly" which has a uniform rate of change. Then with some elementary trigonometry and ellipse geometry, Smart (1962) shows that

$$\tan\frac{v}{2} = \frac{(1+e)^{1/2}}{(1-e)^{1/2}}\tan\left(\frac{E}{2}\right). \tag{12}$$

Furthermore, the radius vector,

$$R_S = a_S(1 - e\cos E), \tag{13}$$

where a_S is the semi-major axis of the ellipse.

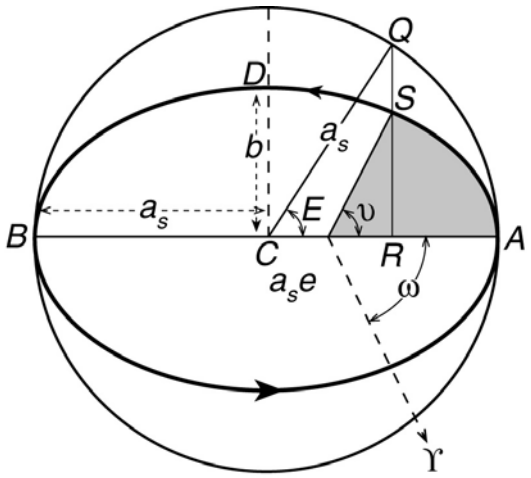

Figure 6: Geometry of a body at S moving in an exaggerated ellipse about the earth at a focus. ν is the true anomaly of the body (the sun), E measured relative to the center of the ellipse is the eccentric anomaly. ω defines the angle between the vernal equinox Υ and perihelion. a_S , b are the semi-major and minor axes of the ellipse, and a_S is also the radius of the bounding circle. ν, E, M (the solar anomalies) are all measured from perigee. M is the angle of the position of the fictitious mean sun moving uniformly along the circle.

– – – – – – – – – – – – – – – –

Define a fictitious mean sun moving at the average angular rate of the real sun at orbital longitude M, the mean anomaly,

$$M = n\,(t - \tau) \tag{14}$$

where τ is a time origin and n is a frequency defined as one cycle/year. Some more elementary geometry and Kepler's Law shows that the relationship between E and M is given by the "Kepler Equation",

$$E - e \sin E = M = n\,(t - \tau)\,. \tag{15}$$

For small e (typically about .02 for the sun), the Kepler Equation can be solved iteratively for E in terms of t, or M; then v is known from (12) , and R_S from (13) . Ignoring all of the details, it is apparent that v and R_S will carry periodicities at one year, 6 months, and all of the higher harmonics of the year and all of these frequencies will further split the basic tidal lines in Eq. (10). Astronomical references give the fundamental parameters as functions of time, typically in Taylor series in terms of Julian Centuries, T, of 36525 days. So for example, Anonymous (1961, p. 98), gives the mean anomaly,

$$M = 358°28'33.00'' + 129596579''.10T - 0.54''T^2 + ... \tag{16}$$

relative to the vernal equinox of 1 January 1950. Note that the mean anomaly is not exactly a uniformly increasing angle with time.

The point marked Υ in Figs. 4, 6 lies along the line of intersection of the plane of the earth's equator and the plane of the ecliptic (the two make an angle of about 23°). The sun crosses the earth's equator twice per year at the equinoxes with the spring or vernal equinox defined as the time when the sun crosses the equator into the northern hemisphere. The point in space toward which the line of intersection is directed is called the "First Point of Aries" or the "vernal equinox". This intersection with the solar orbit is used as a reference point for measuring the time origin. Because the earth's rotation pole precesses in space, with a period of about 26,000 years, the line of intersection moves, westward, completing a 360° rotation in that period of time. For conventional astronomical work over short periods of time, one uses a fixed line, e.g., its position at noon on 1 January 1950 or 1900. The Milankovitch theory commonly uses the position of Υ in 1850, but the geometry can be developed for moving positions.

For solar tides, the only remaining complication is the fact that the orbital ellipse is not quite closed. The point of closest approach of the earth to the sun (perihelion), or of sun to earth (perigee), moves counterclockwise in Fig. 6, in the direction of the solar motion. In an absolute frame, perigee would take about 110,000 years to go through 360°. But the vernal equinox is moving clockwise, towards perigee, and thus relative to Υ, the period is only about 21,000 years.

To obtain a complete description of the solar tidal disturbing potential, V_S/g, one expresses θ_S, λ_S, R_S in terms of M (the mean anomaly, not mass) and notes that everything is periodic involving three frequencies: one cycle/solar day, $1/T_1$, one cycle per year, $1/T_3$, and one cycle per 21,000 years, $1/T_6$ and all of their harmonics. By inspection, one can write

$$\frac{V_S}{g} = \sum_{n_1,n_3,n_6=-\infty}^{\infty} A\left(n_1, n_3, n_6, \theta, \lambda\right) \left\{ \begin{array}{c} \cos\left[2\pi\left(\frac{n_1}{T_1}t + \frac{n_3}{T_3}t + \frac{n_6}{T_6}t\right)\right] \\ \sin\left[2\pi\left(\frac{n_1}{T_1}t + \frac{n_3}{T_3}t + \frac{n_6}{T_6}t\right)\right] \end{array} \right\}. \tag{17}$$

In practice, only small integers, (n_i) are required for very high accuracy (never more than ± 5). The skipped indices are reserved for the moon and will be explained below. Terms with $n_1 = 0$ are termed long-period tides, and the form of their spatial structure is $A\left(0, n_3, n_6, \theta, \lambda\right) = B\left(0, n_3, n_6\right) P_2\left(\cos\theta\right)$, with no longitude dependence. $n_1 = 1$ terms are the diurnal tides, and $A\left(1, n_3, n_6, \theta, \lambda\right) = B\left(1, n_3, n_6\right) P_2^1\left(\cos\theta\right)\left(\cos\lambda,\ \sin\lambda\right)$; for $n_1 = 2$, $A\left(2, n_3, n_6, \theta, \lambda\right) = B\left(2, n_3, n_6\right) P_2^2\left(\cos\theta\right)\left(\cos 2\lambda,\ \sin 2\lambda\right)$. These are the semi-diurnals. $P_l^m\left(\cos\theta\right)$ are the "associated Legendre polynomials of order l, and degree m. (A complete development of the tidal potential is done wholly in spherical harmonics; Eq.(9) is a special case of the "addition theorem" for spherical harmonics.) Other tides exist ($n_3 = 3$ are the ter-diurnals, but are significantly weaker—although they can be observed in the ocean). Fuller derivations and discussion can be seen in the references already given.

Eq. (17) is representative of a more general statement: the gravitational tidal disturbing potential is a non-linear function of the solar radius and angle (orbital anomaly). In common with most non-linear systems, its behavior can be written as a simple sum over the 3 basic frequencies and their simple harmonics; generally, all of the amplitudes rapidly diminish with harmonic number, n_i.

1.3 Lunar Tides

The underlying principle of the lunar tides is identical: one uses a local elliptical approximation to the lunar orbit and the lunar disturbing potential, V_L/g, is the identical expression to (10) with the lunar mass M_L and orbital radius R_L replacing those for the sun, and similarly for the various relative position angles, λ_L, θ_L. Lunar mass is much less than solar mass, but because the disturbing potentials depend upon the cube of the separation between the bodies, the close lunar distance "wins". But the lunar orbital motion is more complicated than for the sun, because the position of the moon depends upon the location of the sun, but the opposite is not true (to a very high degree of approximation) so that one must write terms for the local distortion of the lunar orbital ellipse as the relative sun/moon positions change (e.g., when aligned, the lunar

radius increases slightly)[1]. The lunar orbit is also tilted with respect to both the earth's equator and the plane of the ecliptic so that one has more angles to keep track of. The plane of the lunar orbit precesses with a period of about T_5 =18.6 years, and the perigee point rotates through 360° in a period of about T_4 =8.9 years. But with the addition of these three periods (one cycle/month=$1/T_2$, one cycle/8.6 years, and one cycle/18.6 years), one obtains an expression essentially identical to (17) ,

$$\frac{V_L}{g} = \sum_{n_1,n_3,n_6=-\infty}^{\infty} A\left(n_1, n_2, n_3, n_4, n_5, n_6, \theta, \lambda\right) \left\{ \begin{array}{c} \cos\left[2\pi\left(\sum_{i=1}^{6} \frac{n_i}{T_i} t\right)\right] \\ \sin\left[2\pi\left(\sum_{i=1}^{6} \frac{n_i}{T_i} t\right)\right] \end{array} \right\} \tag{18}$$

with the solar frequencies appearing because they influence the lunar position. There are, once again, long-period (one-month and two weeks periods), diurnal and semi-diurnal groupings, although the "day" is the so-called lunar, rather than solar day.

1.4 Combined Tides

Customarily, one treats the lunar and solar tides together as $V/g = V_L/g + V_S/g$, tabulating them generally in terms of the six numbers n_i. The arguments of the cosines are determined by the 6-tuple (n_1,$n_2, ...n_6$) called the Doodson number (with 5 added in tabulations so as to produce positive numbers). There are details worth knowing about, but these are left to the references. Cartwright and Edden (1973) is the most recent general expansion. Because the lunar tides are stronger than the gravitational ones, compilers of the tidal expansions generally use a mean lunar day rather than the mean solar day. Table 1 (as adapted from Doodson, 1921) gives the nominal frequencies and periods used in mean solar days.

At least two different days, three different years, and four different months can be defined. The frequency of the solar day is $f_1 + f_2$, corresponding to the shorter time interval between zenith passages of the mean sun compared to the mean moon. The tropical year, used in the table, is defined as the interval over which the sun passes successively through Υ; the anomalistic year is the time for successive passages through perigee (and because perigee is moving in the direction of the sun, the anomalistic year is slightly longer. The frequency is evidently $f_3 - f_6$.) Similar relations occur for the differing month definitions; see Anonymous (1961) or Smart (1962).

[1]The orientation of the earth in space, and hence its rotation axis, does depend upon the lunar position, and hence the relative separation of sub-solar point and observer does have lunar terms in it. Thus for example, there is a change in the earth's obliquity forced at the 18.6 year lunar period, and which would introduce such a periodicity into the insolation function.

Label	Name	Frequency (°/mean solar day)	Period (tropical years)
f_1	1 cycle/lunar day	347.81	2.83×10^{-3}
f_2	1 cycle/tropical month	13.18	7.47×10^{-2}
f_3	1 cycle/tropical year	0.986	1.0
f_4	1 cycle/lunar perigee period	0.1114	8.98
f_5	1 cycle/lunar nodal period	0.0529	18.63
f_6	1 cycle/solar perigee period	4.71×10^{-5}	20,940

Table 1: The six frequencies and corresponding periods used in normal tidal work (periods less than 21,000 years). Equally valid use can be made of the solar rather than the lunar day, and of any of the other definitions of a month and year. The time origin is generally measured from the vernal equinox at a fixed date. This table can be extended to lower frequencies to encompass the Milankovitch periodicities below 1 cycle/solar perigee period.

The discussion given thus far is adequate for all ordinary tidal purposes, and indeed the dependence upon f_6 is often ignored (we have no sealevel records approaching such long periods). At much longer periods (as are of interest in the insolation problem), one must account for lower frequencies present in the solar system and for various additional complexity. For example, the earth's eccentricity varies, and can go through zero, leaving perigee undefined. When it re-emerges from zero, the perigee point can be at a very large angle from where it was last defined.

The frequencies f_i are irrational multiples of each other. So by choosing the n_i, possibly using very high values, it is possible to produce with arbitrary accuracy *any* frequency

$$f_d = n_1 f_1 + n_2 f_2 + ... + n_6 f_6, \tag{19}$$

and this possibility has led to a strange numerological literature in which claims are made for important tidal forcing at a variety of periods (e.g., deRop, 1971; Keeling and Whorf, 1997). But if one actually works out the forcing amplitude at that frequency, they almost always turn out to be minuscule and so unimportant. Note that Doodson (1921) shows no line corresponding to f_6 alone—there is no significant energy at the precessional frequency; it is important only in splitting higher frequency tidal lines.

2 Thermal Tides

Munk and Cartwright (1966) recognized that some of the sealevel variability observed at semi-diurnal and diurnal periods was due to meteorological phenomena. For example, the daily heating and cooling of the ocean surface makes the water column expand and contract. In some places there are daily seabreeze effects. To analyze these effects, which otherwise contaminate the analysis of the ocean or earth response to the gravitational disturbances, they defined a thermal or "radiational" tide forcing function. It is at this stage that tidal theory encounters insolation and becomes the Milankovitch problem. They wrote a "radiation function" (I will call it the "insolation function"),

$$\begin{aligned}
\mathcal{R} &= S_0 \left(\frac{\bar{R}_S}{\rho_S} \right) \cos\alpha \\
&= S_0 \frac{\bar{R}_S \cos\alpha}{R_S \left(1 - 2\left(a/R_S\right)\cos\alpha + \left(a/R_S\right)^2 \right)^{1/2}}, \ \cos\alpha > 0 \qquad (20) \\
&= 0, \ \cos\alpha < 0 \qquad (21)
\end{aligned}$$

where α is the same angle appearing in the tidal potential (see Fig. 1), S_0 is the solar constant and $\bar{R}_S$ is the time mean solar distance. One then expands the denominator of (20) as before,

$$\begin{aligned}
\mathcal{R} &= S_0 \frac{\bar{R}_S}{R_S} \cos\alpha \left(1 + \frac{a}{R_S} P_1\left(\cos\alpha\right) + \left(\frac{a}{R_S} \right)^2 P_2\left(\cos\alpha\right) + ... \right), \ \cos\alpha > 0 \qquad (22) \\
&= 0, \ \cos\alpha < 0. \qquad (23)
\end{aligned}$$

The behavior of $\mathcal{R}$ differs from that of V in three ways. (1) It is physically sensible only on $r = a$. (2) The restriction $\cos\alpha > 0$—means that the earth is opaque to radiation and hence only the illuminated hemisphere sees a non-zero $\mathcal{R}$. (3) The $P_1\left(\cos\alpha\right) = \cos\alpha$ term must be retained, as there is no analogue to the centrifugal force which balances this term in the gravitational disturbance. One expands $(22, 23)$ in Legendre functions, taking full account of the vanishing for $\cos\alpha < 0$. The result (Munk and Cartwright, 1966, p. 541) is,

$$\frac{\mathcal{R}}{S_0} = \frac{\bar{R}_S}{R_S} \left\{ \frac{\cos\alpha}{2} + \sum_{n=2,4,6,...} \frac{2n+1}{2} \left[\frac{1(-1)..(3-n)}{2\left(4\right)...\left(2+n\right)} \right] P_n\left(\cos\alpha\right) \right\}, \ 0 \leq \alpha \leq \pi, \qquad (24)$$

and then expression (9) is used to calculate $\mathcal{R}/S_0$ in terms of the solar position. There will evidently be semi-diurnal, diurnal, annual, and perigee frequencies, all of their harmonics and all integer multiple sum and difference frequencies. As with the gravitational tides, one must work out the actual amplitudes at a given frequency to see if the forcing is significant. Note that $\mathcal{R}$ as defined is only an approximation: when the solar center is at the horizon with a setting

sun or rising sun, there is illumination in both hemispheres (no abrupt cutoff with $\alpha = 0$), and the insolation would be influenced by atmospheric thickness changes at large α, among other issues.

3 The Milankovitch Problem

The Milankovitch problem involves calculating Eq. (24), but at periods much longer than conventionally used in tidal analyses. The main issues are finding accurate expressions for $\cos\alpha$ and R_S valid over hundreds of thousands and millions of years. This is a problem of positional astronomy which at long periods must account for the changing disturbances of the other planets, and over sufficiently long periods the system appears to become chaotic.

The clearest developments may be those of Rubincam (1994) or Bills (2001). The positional astronomy (relative separation of observer and sun) remains identical to the treatment above for the radiational tides. The only difference from the treatment of gravity tides and radiational forcing is that one must include changes in the orbital parameters on time scales longer than the conventional tidal cutoff at the perigee period of 21,000 years. The major new elements are the variations in the earth's obliquity (the angle ε_S in Fig.4) and in the eccentricity e. Two phenomena dominate the former: the angle of the rotation axis of the earth varies relative to the normal to the ecliptic (equivalently, the angle between the equator and the plane of the ecliptic), which today is about $23°27'8.26'' - 46.84''T$, that is decreasing, varies between about 22 and 25° degrees, and the plane of the ecliptic itself undergoes a forced motion relative to the so-called invariable plane. The invariable plane is defined as being perpendicular to the net angular momentum axes of the solar system; the motion arises because of interactions of the earth with all the other planets.

Starting with an expression identical to (22), Rubincam (1994) omits all terms dependent upon λ, thus suppressing all of the daily and higher frequency variations, leaving only the long-period terms. He then finds, to lowest order (following a correction, Rubincam (2001, *Black*

body temperature, orbital elements, and the Seversmith Psychroterm, unpublished manuscript),

$$\frac{\mathcal{R}}{S}=\left(\frac{\bar{R}_S}{a_s}\right)^2\left\{\begin{array}{c}\frac{1}{4}P_0\left(\cos\theta\right)\left[1+\frac{e^2}{4}+2e\cos M+\frac{5}{2}e^2\cos 2M\right]+\\ \frac{1}{2}P_1\left(\cos\theta\right)\left[\begin{array}{c}\left(1-\frac{e^2}{2}\right)\sin\varepsilon_S\sin\left(\omega+M\right)+2e\sin\varepsilon_S\sin\left(\omega+2M\right)+\\ \frac{e^2}{8}\sin\varepsilon_S\sin\left(\omega-M\right)+\frac{27}{8}e^2\sin\varepsilon_S\sin\left(\omega+3M\right)\end{array}\right]+\\ +\frac{5}{16}P_2\left(\cos\theta\right)\left[\begin{array}{c}\left(1+\frac{e^2}{2}\right)\left(\frac{3}{4}\sin^2\varepsilon_S-\frac{1}{2}\right)-\frac{3}{4}\left(1-\frac{7}{2}e^2\right)\sin^2\varepsilon_S\cos\left(2\left(\omega+M\right)\right)\\ +2e\left(\frac{3}{4}\sin^2\varepsilon_S-\frac{1}{2}\right)\cos M+\frac{3}{4}e\sin^2\varepsilon_S\cos\left(2\omega+M\right)\\ -\frac{9}{4}e\sin^2\varepsilon_S\cos\left(2\omega+3M\right)+\frac{5}{2}e^2\left(\frac{3}{4}\sin^2\varepsilon_S-\frac{1}{2}\right)\cos 2M\\ -\frac{39}{8}e^2\sin^2\varepsilon_S\cos\left(2\omega+4M\right)+...\end{array}\right]\end{array}\right. \tag{25}$$

Here, M is again the true anomaly, ω the angle of perigee, a_s is the semi-major axis of the solar orbit. Any terms having M in the argument will average to zero over the course of a year; thus by eliminating them, one can isolate the insolation changes at periods longer than a seasonal cycle, in which case Eq. (25) reduces to,

$$\left.\frac{\mathcal{R}}{S}\right|_{NS}=\left(\frac{\bar{R}_s}{a_s}\right)^2\left\{\frac{1}{4}\left[1+\frac{e^2}{4}\right]+\frac{5}{16}P_2\left(\cos\theta\right)\left(1+\frac{e^2}{2}\right)\left(\frac{3}{4}\sin^2\varepsilon_S-\frac{1}{2}\right)\right\}, \tag{26}$$

so that the only non-seasonal effects enter from the variations of eccentricity e, and obliquity, ε_S. Because e is very small, and appears to remain so over the history of the solar system, the dominant non-seasonal forcing arises from ε_S. A Fourier analysis of (26) as computed by Bills (2001) is shown in Fig. 7. One sees energy around 41,000 years period, albeit split into several nearby frequencies, as one has come to expect. There is a very slight peak near 100,000 years owing to variations in e near that period.

Expression (26) is not completely intuitive. The fundamental geometric effect is the dependence of changes insolation upon $\rho_S^{-2}, \rho_S^{-3}, ...$, the earth-observer distance. Averages over a year of ρ_S^{-2}, etc. differ, depending upon the latitude and inclination of the observation point. If the inclination is large, with $3/4\sin^2\varepsilon_S > 1/2$, then because $P_2\left(\cos\theta\right)=\left(3/2\right)\cos^2\theta-1/2<0$ on the equator ($\theta=\pi/2$), the contribution is negative and hence there is reduced tropical insolation compared to the poles. At the limit, $\varepsilon_S=\pi/2$, the sun is in a polar orbit about the earth. If $\varepsilon_S=0$, the equator has enhanced insolation relative to the poles. The two effects, polar amplification, and equatorial amplification just compensate when $3/4\sin^2\varepsilon_S-1/2=0$, or near 54°. With an actual inclination near 23°, the mean effect is to enhance tropical insolation, and the time variability of ε_S modulates the intensity of this difference, changing the annual mean radiation as a function of latitude. Hence obliquity variation has a direct effect on the intensity of the received radiation.

Rubincam (1994) makes the extremely important point that to the extent the climate system responds linearly to variations in $\mathcal{R}$, only the obliquity variations near 41,000 years period are

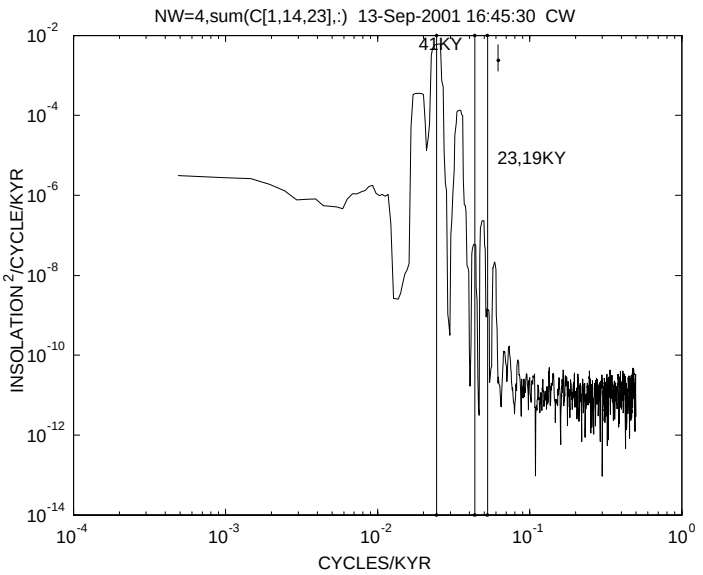

Figure 7: Power density spectrum of the long period terms in insolation, Eq. (26) from a calculation of duration 2 MY sampled at intervals of 1KY. Vertical lines show the dominant obliquity period of 41KY and the two main precessional terms at 23 and 19KYR. The latter are essentially absent in a year-long average. The eccentricity term at 100KY is very small. (From a time series of B. Bills, 2001)

———————————————

expected to produce climate change. In particular, the terms in (25) with periodicities involving the precession, e.g. $\sin(\omega + M)$, vanish if averaged over a period near one year, and can only appear in the climate system if some element in it responds to the amplitude of the seasonal cycle. That is to say, all forcing terms like $\sin(\varepsilon_S)\sin(\omega + M)$ lie very close to the frequency dM/dt, that is, a cycle/year. If the response is observed instead, near frequency $d\omega/dt$, one has somehow rectified the annual cycle: such a response is non-linear. In a linear system, the response would be confined to frequencies very near $d(\omega + M)/dt \approx dM/dt$, and nothing would be visible near $d\omega/dt$. This point does not seem to have been widely appreciated. It is consistent with the absence of an f_6 frequency line in the tidal development.

One way of retaining the dependence on ω despite the vanishing of the seasonal average, is to postulate a dependence upon the value of the insolation at a particular time of year, e.g., that the growth of an ice sheet depends only upon the insolation in the summer months, or over some particular month or fraction of a year. Such a response is intrinsically non-linear, as it corresponds to a rectifier in what is sometimes known as a $\nu-$th law device. One algebraic representation is to postulate that the response to the sinusoidal forcing is of the form,

$$\begin{aligned} y(t) &= |\cos\omega\cos M|^{\nu},\ \cos(\omega + M) > 0, \\ &= 0,\ \cos(\omega)\cos(M) < 0. \end{aligned} \tag{27}$$

As $\nu \to \infty$, $y(t)$ is dependent primarily upon the maximum value of the cosine. Such rules are analyzed in detail by e.g., Davenport and Root (1958), or Middleton (1960). The main point is that a dependence upon seasonality in producing a precessional period requires a non-linear system. In such a system, one would anticipate specific structures in the spectrum as clues to the physics. Simple rules such as Eq. (27) produce a dominant low frequency response at the first harmonic, 2ω, rather than at ω, but related systems exist with response at or near ω, for example by considering the rule

$$\begin{aligned} y(t) &= |(1 + a_1\cos\omega)\cos M|^{\nu},\ \cos(\omega + M) > 0, \\ &= 0,\ (1 + a_1\cos\omega)\cos M < 0, \end{aligned} \tag{28}$$

where $a_1 < 1$ is a constant. Such a rule would more realistically represent an insolation curve in which the dependence on ω was a perturbation on top of a mean seasonal cycle.

Unfortunately however, any recording device with a similar response will produce purely *apparent* rectified signals. Consider for example, coccoliths or diatoms, other biological elements whose growth, $q(t)$, occurs only in summer months. Then $y(t)$ will obey a rule analogous to (27), perhaps modified by the requirement of a minimum threshold greater than 0, and there will then be low frequencies present in the geological record having nothing to do with the climate

signals themselves, and reflecting only the recording device. Such possibilities present serious complications to the analysis of climate change: consider e.g., loess deposits which only occur when the wind speed and duration exceed certain thresholds.

4 Analysis

Serious tidal analysis in modern form began in the Nineteenth Century and is associated with the names of Whewell, Kelvin, etc. (see Cartwright, 1999). The relevance for the Milankovitch problem is that tidal analysis long ago confronted the problem of understanding forced, strictly periodic motions, in the presence of other motions usually best described as random or stochastic. The experience, and tools developed, are thus directly relevant for understanding forced insolation changes, up to the differences in the nature of the forcing. Tidal signals exist in almost every geophysical time series from the ionosphere to temperature changes at the bottom of the ocean to the deformation of the earth. In many of these records, the tidal motions are relatively weak, and one may have to work hard to extract them. In sealevel, the most studied of tidal records, often 99% of the variance lies in the tidal bands, depending upon the record lengths, (see Wunsch and Stammer, 1998), and one has an unusual and (for the tidal analyst) happy situation of a very large signal-to-noise ratio.

There are two basic approaches to understanding tidal signals in records of any sort, no matter what the signal-to-noise ratio: (1) in the frequency domain, and (2) in the time domain. The approaches are completely equivalent, able to produce identical information (see, e.g., Wunsch, 2000). The main differences are those of convenience, in the implementation of numerical analysis algorithms, in the ease with which one can impose various a priori physical constraints on the analysis, and then interpret the result.

4.1 Frequency Domain Analysis

Historically, frequency domain analysis emerged first (associated largely with Lord Kelvin), and it remains today the most widely used, and more readily physically interpretable approach. The physical interpretation is accessible because most of us tend to think of many physical phenomena as characterized by their basic frequencies, and we expect physics to be different in different frequency bands (e.g., high frequency ripples on the ocean surface have a different set of governing equations than does low frequency swell). Beyond that, the hypothesis of linearity of a physical system says that if one forces a linear system at a frequency s, then the response will occur only at that same frequency, with at most an amplitude and phase shift relative to the forcing. For ocean tides (and most tides in the real world), this is an excellent first

approximation; it does fail in some places.

The tidal forcing potential Eq. (10) says the forcing of the ocean (I will speak of the ocean, but the comments apply to any part of the geophysical system), can be regarded as a linear sum of pure frequencies, s_i given by the Doodson numbers and with an amplitude one can either look up in published tables, or (these days), obtain numerically from a computer. The forcing has some amplitude, $H(s_i)$ and phase, $\eta(s_i)$, which we can, without any loss of generality take to be zero (simply implying a shift in time origin). The hypothesis of linearity asserts that the ocean response will be at this same frequency, with amplitude $A(s_i)$, and phase $\gamma(s_i)$. The amplitude and phase will depend upon the physical variable being analyzed (surface elevation, water velocity, temperature, pressure, etc.). We learn about the ocean by trying to understand, from the equations of motion of the fluid, why $A/H, \gamma - \eta$ have their particular values and how and why they vary with frequency and location.

In pre-computer days, clever algorithms for hand calculation were developed to minimize the huge analysis labor (see Schureman, 1958). Today, computers rapidly calculate A, γ from long records. The process is related to, but somewhat different from, ordinary Fourier analysis, simply because the tidal frequencies are not integer multiples of each other, and one has to modify the usual procedures (there are several ways to do that). Complications arise in a number of ways. One important one is the need to account for the presence in A, γ of contributions otherwise present in the ocean, but unrelated to the tides themselves.

Because the tidal forcing contains nearby frequencies, they are often not "resolved", that is separated from each other in frequency (see Wunsch, 2000, or any book on Fourier analysis). Unseparated lines will have an apparent amplitude and phase dependent upon the relative amplitudes and phases of the unseparated frequencies, as well as the actual time interval being analyzed, and one must correct for the effect. Consider the sum of two nearby sinusoids,

$$\begin{aligned} & H_1 \sin 2\pi s_1 t + H_2 \sin\left[2\pi\left(s_1 + \Delta s\right) t - \eta\right], \ \Delta s/s_1 << 1 \\ = \ & A \sin\left(2\pi s_1 t - \beta\right), \qquad (29) \\ A \ = \ & \left\{H_1^2 + H_2^2 + H_1 H_2 \cos\left(2\pi \Delta s t - \eta\right)\right\}^{1/2}, \\ \beta \ = \ & -\arctan\left(H_2 \sin\left(2\pi \Delta s t - \eta\right) / \left(H_1 + H_2 \cos\left(2\pi \Delta s t - \eta\right)\right)\right) \qquad (30) \end{aligned}$$

that is, with a slowly (depending upon Δs), changing amplitude and phase. Standard tabulations left the 18.6 year-nodal regression terms unresolved, and d tabulated the slowly changing A, β as the apparent amplitude and phase (called f, u) of the unresolved lines (Schuremann, 1958).

The other issue is that the physics could conceivably change in the small frequency interval Δs, e.g., owing to a resonance (these exist, but are comparatively rare in the real ocean).

The Milankovitch forcing has been treated, generally, in similar frequency domain ways.

It helps to have a slightly more general notation. Let $\zeta(t)$ be any physical variable thought to exhibit tidal or Milankovitch responses. Denote the Fourier transform of any variable by a carat, e.g. the Fourier transform of $\zeta(t)$ is $\hat{\zeta}(s)$ where s is the frequency. Let $h(t)$ be either Milankovitch or tidal forcing, or the sum of the two. Then the hypothesis of a linear response is readily shown to be equivalent to,

$$\hat{\zeta}(s) = \hat{p}(s)\,\hat{h}(s), \tag{31}$$

so that the response at frequency s, multiplies the forcing by an amplitude $|\hat{p}(s)|$ and shifts it by a phase $\beta(s) = \tan^{-1}\left[\mathrm{Im}\left(\hat{p}(s)\right)/\mathrm{Re}\left(\hat{p}(s)\right)\right]$, where Im, Re denote the real and imaginary parts of $\hat{p}(s)$. No other relationship is consistent with the linearity hypothesis. $\hat{p}(s)$ is sometimes called the admittance or "transfer admittance" function. $P(s_i) = |\hat{p}(s_i)|\exp(\beta(s_i))$. Understanding the relationship between Milankovitch and/or tidal forcing and the system response can be viewed as an attempt to find the transfer function. A limitation is that as we have seen $\hat{h}(s)$ only has non-zero amplitude in rather narrow frequency bands surrounding the basic astronomical frequencies. An explicit attempt to find a transfer function can be seen in Wunsch (1972).

4.2 Time Domain Analysis

The hypothesis that the system response to an arbitrary forcing is a linear one has the time domain equivalent of (31), which is,

$$\zeta(t) = \int_{-\infty}^{\infty} p\left(t'\right) h\left(t - t'\right) dt', \tag{32}$$

that is, a "convolution". In most data analysis with computers, one uses sampled functions, at intervals Δt and writes (32) as a summation[2],

$$\zeta(n\Delta t) = \sum_{m=-\infty}^{\infty} p(m\Delta t)\, h(n\Delta t - m\Delta t), \tag{33}$$

or more concisely,

$$\zeta_n = \sum_{m=-\infty}^{\infty} p_m h_{n-m}. \tag{34}$$

In practice, one cannot run sums to infinity, and there is no need to. The problem of understanding the behavior of a linear system then becomes that of finding approximating values p_m. The equivalence of (34 and 31) follows from the "convolution theorem", which asserts that the

[2] There are various dimensions (units) to keep track of in moving from an integral to a sum. Often one sets $\Delta t = 1$, suppressing the units, but they come back to haunt one eventually.

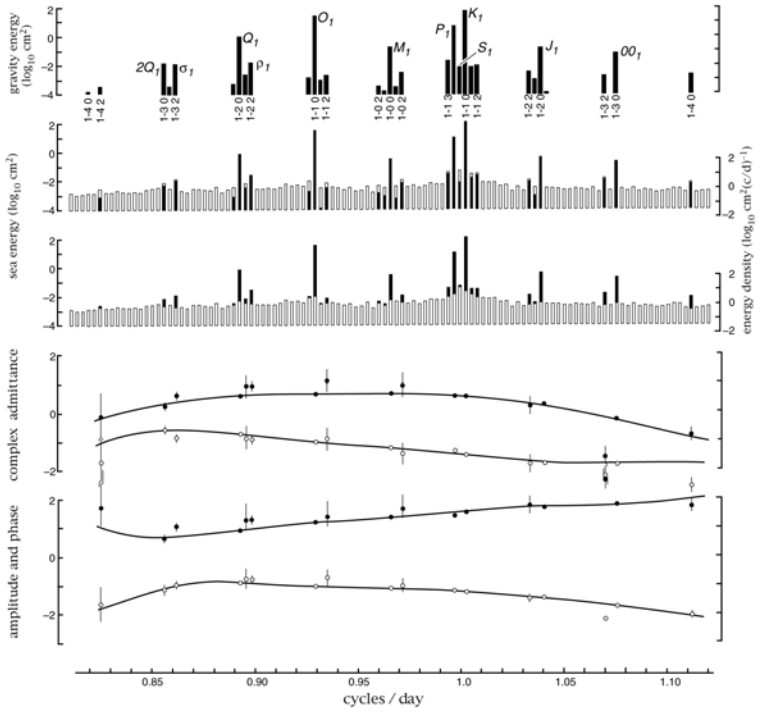

Figure 8: From Munk and Cartwright (1966) showing the diurnal band frequencies separable at one cycle/year as well as an analysis of the behavior of the tides at Honolulu (see the text). None of the frequencies lies very far from 1 cycle/lunar or solar day.

Fourier transform of a convolution sum as on the right of (34) is the product of the Fourier transforms of the two functions appearing (see e.g., Wunsch, 2000).

Several ways exist to determine the p_m in (34) using finite upper and lower limits (which must be determined). The most straightforward way is through ordinary least-squares, finding the minimum over p_m of,

$$\delta^2 = \sum_{n=-N_1}^{N_2} \left(\zeta_n - \sum_{m=-N_1}^{N_2} p_m h_{n-m} \right)^2 . \tag{35}$$

The standard reference on this subject is Munk and Cartwright (1966) who discuss choices of Δt, N_1, N_2, etc.

As a summary statement, Figs. 8, 9 show an analysis by Munk and Cartwright (1966) in both frequency and time domains of the tide gauge record at Hawaii. The uppermost panel in each figure shows the energy in the diurnal and semi-diurnal bands respectively, the first proportional

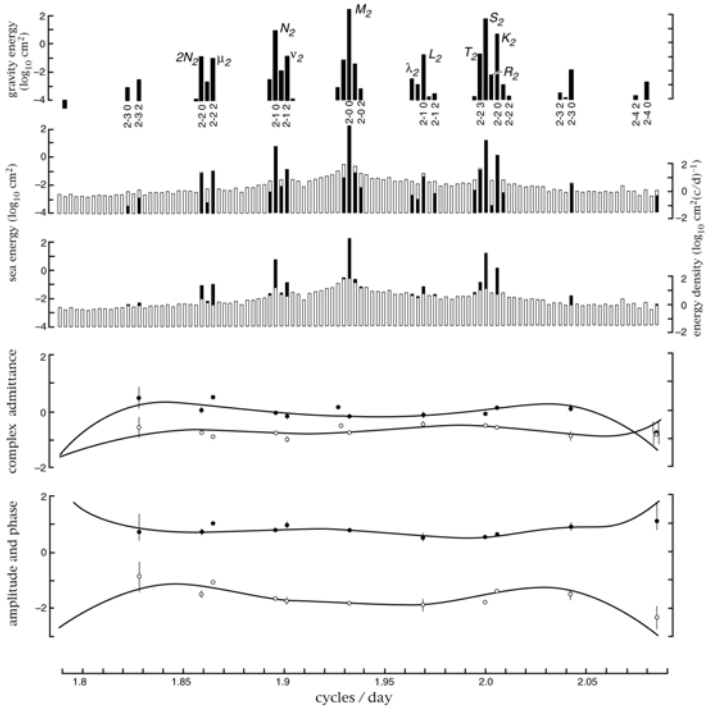

Figure 9: Same as Fig. 8 except in the semi-diurnal band (note the frequency scales in the two figures). See text for explanation of the various panels.

to the spherical harmonic $P_2^1(\cos\theta)(\cos\lambda, \sin\lambda)$, the second to $P_2^2(\cos\theta)(\cos 2\lambda, \sin 2\lambda)$. Note the clustering (the clusters are separated by multiples of a cycle/month, and within the clusters, they are separated by multiples of one cycle/tropical year) and the large frequency gap between the diurnals and semi-diurnals. Lines separated by multiples of one cycle/8.9 years or 18.6 years are unresolved here. The 2nd and 3rd panels from the top show the "coherence"-squared between the forcing (V/g) and the tide gauge record. The black bar shows the coherent part (the fraction of the variance explained by the forcing in that frequency band). Two plots are required because in a logarithmic display one cannot show additive powers and if one or the other of the coherent or incoherent power is much less than the other, it will be visible on only one of the two plots. The lowest panel shows the estimated $|\hat{p}(s)|, \beta(s_i)$ at Honolulu, and the panel above displays the equivalent real and imaginary parts of $\hat{p}(s)$. Points indicate the frequencies of actual tidal energy. The smooth curves are obtained by making assumptions about the behavior of p_m; see Munk and Cartwright (1966) for details. These lower curves were first obtained in the time domain from Eq. (35), and then Fourier transformed to obtain the figures. Generally speaking, most people find the frequency domain representation easier to understand, even when the time domain method is used.

The time domain method has a number of virtues and will probably become the method of choice for testing the Milankovitch hypothesis in cores, but the effort is only starting. There is one variant on what Munk and Cartwright (1966) called their "response method". If one solves the least-square problem of minimizing δ^2, the coefficients so estimated, p_m, tend to be very sensitive functions of N_1, N_2 although their Fourier transforms are more stable and interpretable. Groves and Reynolds (1975) suggested working with an orthogonalized set of p_m, a suggestion explored by Alcock and Cartwright (1978), with some degree of success. Bills (2001) starts the use of this method in the Milankovitch problem.

5 Detection of Non-Linearities

As noted above, the existence of precessional effects in the climate system appears to require important non-linearities in the response to insolation. Furthermore, many of the rationalizations of the 100KY response in the climate system demand non-linear interactions. One thus is driven to understand the extent to which the records display non-linear characteristics, and in what form.

As with non-linear systems in general, techniques for analysis tend to be more ad hoc and less general than methods characterizing linear systems, partly because the nature of possible non-linearities is so wide. In geophysics in the widest sense, as with most mathematical approaches,

one hopes to begin with an assumption of weak non-linearity, so that perturbation methods can be used. As written, Eq. (27, 36) represent a fully-non-linear response, but if we modified 27 to,

$$\begin{aligned} y(t) &= A\cos\left[(\omega+M)t-\beta\right]+\delta\left|\cos(\omega+M)t\right|^{\nu},\ \cos(\omega+M)t>0, \\ &= A\cos\left[(\omega+M)t-\beta\right],\ \cos(\omega+M)t<0,\ \delta<<1, \end{aligned} \tag{36}$$

the response has a linear component. Note that the modern climate system does have, in some elements, a major seasonal response, which is mimicked by (36). One might hope to determine the magnitude of δ.

A few general techniques exist. To the extent that the frequency function (probability density) for a time sequence y_t is Gaussian, there is prima facie evidence of a linear system, because if the input to a linear system is Gaussian (normal), it is readily shown to remain normally distributed. Here "normal" would carry over to the joint probability density as well, $p\left(y(t),y(t'),y(t'''),...\right)$. Various tests exist for significant deviation from normality. Of course, if the input function is itself non-normal, then nothing is proved about the system by a failure to be non-normal, and one is driven to understand the transformation of the probability density by passage through the climate system, if possible.

Because the physics of the system changes with frequency, one often seeks non-linearity as a function of frequency. Consider that for a stationary Gaussian time series, a complete statistical description is contained in the mean, and the second moments $R(\tau) =< y(t)\,y(t+\tau) >$. The Fourier transform of the autocovariance, $R(\tau)$ is just the power density spectrum (by the Wiener-Khinchin Theorem). The latter can be written as

$$\mathcal{F}(R(\tau)) = \Phi(s) \propto \langle \hat{y}(s)\,\hat{y}(s)^{*}\rangle$$

Here, $\mathcal{F}$ denotes the Fourier transform, $*$ is the complex conjugate, and the brackets indicate expected value. Hence the mean, and the ordinary power density spectrum completely describe a (jointly) Gaussian time series. But if the process is not Gaussian (and, a complication, if it is not stationary), the power density is no longer a complete description of the time series. One is led to compute the higher order moments

$$\langle \hat{y}(s_1)\,\hat{y}(s_2)\,\hat{y}(-(s_1+s_2))\rangle. \tag{37}$$

These quantities, usually called the bi-spectrum can be shown to vanish for a Gaussian process (see Hasselmann et al., 1963; Haubrich, 1965, Elgar and Sebert, 1989, among others). As with an ordinary cross-power, the behavior of the bispectrum is complicated by variations in the

magnitude of $\hat{y}(s)$ with s, and one is led to normalize it to the "bicoherence",

$$C(s_1, s_2) = \frac{\langle \hat{y}(s_1)\, \hat{y}(s_2)\, \hat{y}(s_1+s_2)^* \rangle}{\left\{ \left\langle |\hat{y}(s_1)\, \hat{y}(s_2)|^2 \right\rangle \left\langle |\hat{y}(s_1+s_2)|^2 \right\rangle \right\}^{1/2}}. \tag{38}$$

Eqs. (37, 38) represent estimates of the third moments. Tri-spectra, involving fourth moments, and even higher moment spectra may also be required and be informative.

Time domain methods also exist. Suffice it for the moment to point out that simple generalized autoregressive models, e.g.,

$$y_t = a y_{t-1} + b y_{t-1}^2 + \theta_t$$

are possible, with an infinite number of variations.

....

References

Alcock, G. A. and D. E. Cartwright, 1978: Some experiments with "orthotides". *Geophys. J. R. Astronom. Soc.,* 54, 681-696.

Anonymous, 1961: *Explanatory Supplement to The Astronomical Ephemeris an The American Ephemeris and Nautical Almanac.* Her Majesty's Stationery Office, London, 533pp.

Bills, B. G., 2001: Fourier, Legendre, and Milankovitch: searching for the connection between insolation and climate. Unpublished manuscript.

Bowditch, N., 1962: *American Practical Navigator.* United States Government Printing Office, Washinton, 1524 pp.

Cartwright, D. E. and A. C. Edden, 1973: Corrected tables of tidal harmonics. *Geophys. J. Roy. Astron. Soc.*, 33, 253-264.

Cartwright, D. E., 1999: *Tides. A Scientific History.* Cambridge Un. Press, Cambridge, 292 pp.

Darwin, G. H., 1962: *The Tides and Kindred Phenomen in the Solar System.* W. H. Freeman, San Francisco, 378 pp.

Davenport, W. B. Jr. and W. L. Root, 1958: *An Introduction to the Theory of Random Signals and Noise*, 393 pp., McGraw-Hill, New York

Doodson, A. T., 1921: The harmonic development of the tide-generating potential. *Proc. Roy. Soc., A,* 100, 305-329.

Elgar, S. and G. Sebert, 1989: Statistics of bicoherence and biphase. *J. Geophys. Res.,* 94, 10,993-10,998.

Green, R. M., 1985: *Spherical Astronomy.* Cambridge Un. Press, Cambridge, 520pp.

Groves, G. W. and R. W. Reynolds, 1975: An orthogonalized convolution method of tide prediction. *J. Geophys. Res.,* 80, 4131-4138.

Hasselmann, K. W. Munk and G. MacDonald, 1963: Bispectra of ocean waves, in *Time Series Analysis,* M. Rosenblatt, Ed., pp. 125-139, John Wiley, New York.

Haubrich, R. A., 1965: Earth noises, 5 to 500 millicycles per second, 1, *J. Geophys. Res.,* 70,1415-1427.

Imbrie, J. and K, P. Imbrie, 1986: *Ice Ages. Solving the Mystery.* Harvard Un. Press, Cambridge, 224 pp.

Keeling, C. D. and T. P. Whorf, 1997: Possible forcing of global temperature of the oceanic tides. *Proc. Natl. Acad. Scis., USA*, 94, 8321-8328.

Lamb, H., 1932: *Hydrodynamics*, Sixth ed. Dover, New York, 738pp.

Middleton, D. M., 1960: *Statistical Communication Theory,* McGraw-Hill, New York.

Munk, W. H. and D. E. Cartwright, 1966: Tidal spectroscopy and prediction. *Phil. Trans. Roy. Soc., A*, 259, 533-581.

de Rop, W., 1971: A tidal period of 1800 years. *Tellus*, 23, 261-262.

Rubincam, D. P., 1994: Insolation in terms of Earth's orbital parameters. *Theor. Appl. Climatol.*, 48, 195-202.

Schureman, P., 1958: *Manual of Harmonic Analysis and Prediction of Tides,* U. S. Dept. of Commerce, Special Publication No. 98, 317 pp.

Smart, W. M., 1962: *Textbook on Spherical Astronomy*, Fifth Ed. Cambridge Un. Press, Cambridge, 430 pp.

Wunsch, C., 1972: Bermuda sea level in relation to tides, weather, and baroclinic fluctuations. *Revs. Geophys.*, 10, 1-49.

Wunsch, C., 2000: *Time Series Analysis. A Heuristic Primer.* Unpublished classnotes. See http://puddle.mit.edu/ cwunsch/C-12.864/C-12.864.html.

Wunsch, C. and D. Stammer, 1998: Satellite altimetry, the marine geoid and the oceanic general circulation. *Ann. Revs. Earth Plan. Scis.*, 26, 219-254.